Scientia Pharmaceutica

ÖSTERREICHISCHE PHARMAZEUTISCHE GESELLSCHAFT

MDPI

Article

Synthesis and Biological Evaluation of Some Coumarin–Triazole Conjugates as Potential Anticancer Agents

Anarkul S. Kishkentayeva [1,*], Mohammad Saleh Hamad [2], Mikhail A. Pokrovsky [2,3], Zhanar R. Shaimerdenova [1], Aigerim S. Adekenova [1], Gulnara K. Mambeterzina [1], Victor A. Savelyev [3], Andrey G. Pokrovsky [2] and Elvira E. Shults [3,*]

[1] School of Pharmacy, Medical University of Karaganda, Karaganda 100012, Kazakhstan; arsenzhan@bk.ru (Z.R.S.); aika_as.87@mail.ru (A.S.A.); gukema@mail.ru (G.K.M.)
[2] Zelman Faculty for the Medicine and Psychology, Novosibirsk State University, Pirogova Str., 1, 630090 Novosibirsk, Russia; m.khamad@g.nsu.ru (M.S.H.); miha.pokrovsky@gmail.com (M.A.P.); agpok@inbox.ru (A.G.P.)
[3] Vorozhtsov Novosibirsk Institute of Organic Chemistry, Siberian Branch of the Russian Academy of Sciences, 630090 Novosibirsk, Russia; vicsav@nioch.nsc.ru
* Correspondence: anar_kish@mail.ru (A.S.K.); schultz@nioch.nsc.ru (E.E.S.)

Abstract: Despite the discovery of many chemotherapeutic drugs that prevent uncontrolled cell division processes, the development of compounds with higher anticancer efficacy and a lower level of side effects is an important task in modern pharmaceutical chemistry. Herein, a mild and convenient method for the preparation of N1-substituted 3-(1,2,3-triazolyl-methoxycarbonyl)coumarins or *bis*(coumarine-3-carboxylate)*bis*(triazole)alkandiyl by the copper(I)-catalyzed Huisgen cycloaddition reaction of readily available coumarin-3-carboxylic acid propynyl ester with azides or diazides has been presented. The synthesized compounds have been tested for their cytotoxicity on various cancer and noncancerous cell lines using the MTT assay. All new compounds were nontoxic on normal epithelial VERO cells. Two derivatives exhibited selectivity towards HPV-negative human cervical cancer cells, C33 A, with excellent activities in low concentrations (GI_{50} 4.4–7.0 μM). In vitro mechanistic studies showed that bis(coumarine)bis(triazolylester) conjugate **3** induced time-dependent apoptosis in cervical cancer cell lines C33 A and CaSki, at the GI_{50} concentration, as measured by Annexin V-FITC/PI staining. The most active coumarin–triazolyl ester conjugate **2g** possessed anticancer activities, as indicated by its ability to induce S/G2 phase cell cycle arrest at a low concentration and early apoptosis in CaSki cells. The obtained results revealed the potential of new compounds as anticancer agents, particularly against cervical cancer.

Keywords: coumarin-3-carboxylic acid; alkyne; azides; triazoles; CuAAC reaction; cytotoxicity; anticancer agents

check for updates

Academic Editor: Murali Mohan Yallapu

Received: 10 January 2025
Revised: 6 March 2025
Accepted: 23 March 2025
Published: 31 March 2025

Citation: Kishkentayeva, A.S.; Hamad, M.S.; Pokrovsky, M.A.; Shaimerdenova, Z.R.; Adekenova, A.S.; Mambeterzina, G.K.; Savelyev, V.A.; Pokrovsky, A.G.; Shults, E.E. Synthesis and Biological Evaluation of Some Coumarin–Triazole Conjugates as Potential Anticancer Agents. *Sci. Pharm.* **2025**, *93*, 16. https://doi.org/10.3390/scipharm93020016

Copyright: © 2025 by the authors. Published by MDPI on behalf of the Österreichische Pharmazeutische Gesellschaft. Licensee MDPI, Basel, Switzerland. This article is an open access article distributed under the terms and conditions of the Creative Commons Attribution (CC BY) license (https://creativecommons.org/licenses/by/4.0/).

1. Introduction

Coumarin represents a core structural motif that is widely present in natural and synthetic pharmaceuticals [1] and small-molecule fluorescent chemosensors [2]. The synthesis and functionalization of coumarins have given rise to much interest from the synthetic community over the past two decades [3]. Among various coumarins, 3-substituted compounds have attracted significant attention due to their important applications in medicine and chemical biology [4]. Several anticoagulant drugs belong to 3-substituted coumarins [5,6]. Among these compounds, derivatives of coumarin-3-carboxylic acid deserve attention

as inhibitors for certain kallikreins, serine protease, α-chymotrypsin, human leukocyte elastase, and matriptase [7]. The structure–activity analysis of derivatives listed in Figure 1 allows us to determine their importance. Therefore, the anti-inflammatory activity of coumarin esters (general structure **A**) that acted as inhibitors of the kallikrein-related peptidase 9 (KLK9) involved in inflammatory processes of the skin was reported [8]. The anticoagulant and anti-thrombosis agents **B** and **C** (Figure 1) with coumarin ester structures were synthesized using a fragment-based drug discovery approach. Compound **B** was characterized as an inhibitor of the trypsin-like enzymes factor Xa and thrombin [9], as well as coumarin **C, which** represented a perspective group of inhibitors of factor XIIa (*Ki* value of 62.2 nM on FXIIa), a promising target for artificial surface-induced thrombosis and different inflammatory diseases [10]. Coumarin-thiazolyl ester derivatives **D** exhibited a bacteriostatic effect with MIC values of 4 μg/mL, which were characterized as potential bactericides targeting DNA gyrase enzymes (IC_{50} inhibition values of 0.13 μM) and were effective against resistant bacterial strains and biofilms [11]. On the base of coumarin 3-carboxylic acid, some hybrid compounds with a furoxan moiety were synthesized as perspective anticancer agents. Thus, the compound of type **E** exerts strong effects against the breast cancer MDA-MB-231 and 4T1 BC lines ($IC_{50} \leq 1.0$ μM) but show relatively weak cytotoxicity ($IC_{50} \geq 10$ μM) toward healthy MCF-10A (normal cell lines), indicating its excellent selectivity profile [6]. In addition, hybrid **E** generate nitric oxide (NO) in substantial quantities in MDA-MB-231 breast cancer cells, inhibited colony formation, and cause cell death via apoptosis without causing cell cycle arrest [12]. Hybrid compound **F** showed strong antiproliferative activity against human cancer cell lines A549, HT-29, HepG2 and MCF-7 (IC_{50} = 2.10–7.22 μM) and was nontoxic toward normal LO_2 cells (IC_{50} > 50 μM). A preliminary in vivo study of this compound in mice indicates that it is well tolerated, evidenced by zero mortality and normal body weight gains in treated mice [13].

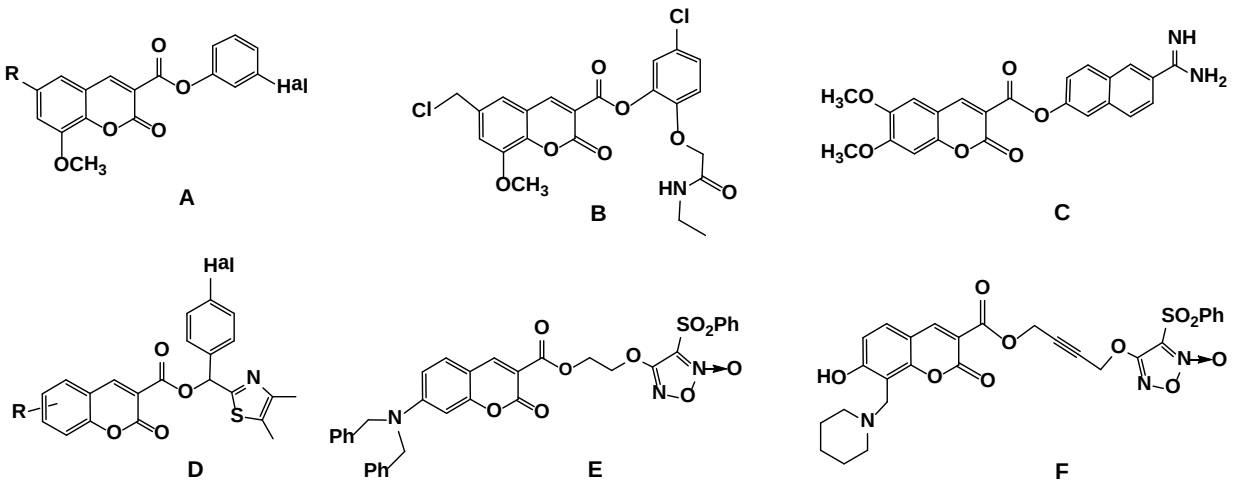


Figure 1. Reported coumarin ester derivatives (structures **A**–**F**) as prototypes for the rational design of the target compounds.

1,2,3-Triazoles scaffold is well known for its pharmacological properties, which could play a major role in the common mechanisms associated with various disorders like cancer, inflammation and neurodegeneration. Triazoles are characterized by low toxicity and superior pharmacokinetics due to the structure of five-membered heterocycles and abundant electron cloud density. As a heteroaromatic motif, the 1,2,3-triazole structure can interact with multiple aromatic amino acids in the receptor–ligand binding process, preferentially engaging with the enzyme binding site [14–17]. Triazole rings mostly act as linkers between various heterocyclic motifs in molecular hybrids. Because of the large dipole moment, 1,2,3-triazoles can act as hydrogen bond donors, mimicking the amide

functional group. More importantly, they are resistant to metabolic degradation and hydrolysis and are stable under acidic, basic and redox conditions in living biological systems [18]. Small molecules with the structure of coumarin–1,2,3-triazole conjugates have been extensively exploited in the molecular design of different derivatives in an attempt to access new molecules with improved anticancer profiles [18–23].

Based on the research literature and our previous work on the structural modification and bioscreening of coumarin–triazole hybrids as antibacterial [24], anticoagulant [25] and anticancer [26] agents, herein, we focused on the synthesis and analysis of the anticancer potential of 3-triazolylmethoxycarbonyl-substituted coumarins and 3,3′-substituted *bis*(coumarino-1,2,3-triazolyl) derivatives obtained from readily available coumarin-3-carboxylic acid **1**. The new series of 1,2,3-triazolyl-modified coumarins was evaluated for their in vitro anticancer activity against human cancer cell lines using the conventional MTT assay. All compounds were nontoxic towards normal epithelial VERO cells and showed differential effects against the tested cell lines, exhibiting a greater impact against the cervical cancer cell lines, especially on the HPV-negative human cancer cells C33 A, and caused cell death by the induction of apoptosis in cervical cancer cells C33 A and CaSki.

2. Materials and Methods

2.1. Materials and Instrumentations

The melting points were determined using thermosystem Mettler Toledo FP900 (Columbus, OH, USA). ^{1}H NMR and ^{13}C NMR spectra were recorded by using a Bruker AV-300 [300.13 (^{1}H), 75.48 MHz (^{13}C)], AV-400 [400.13 (^{1}H), 100.78 MHz (^{13}C)] or DRX-500 [500.13 (^{1}H), 125.77 MHz (^{13}C)] spectrometer. Deuterochloroform ($CDCl_3$) was used as a solvent, with residual $CHCl_3$ (δ_H = 7.24 ppm) or $CDCl_3$ (δ_C = 77.0 ppm) being employed as the internal standard. ^{1}H NMR and ^{13}C NMR spectra for compound **2g** were recorded in DMSO-d_6 by using DMSO-d_6 as the reference standard (δ_H = 2.50 and δ_C = 39.5 ppm). NMR signal assignments were carried out with the aid of a combination of 1D and 2D NMR techniques that included ^{1}H, ^{13}C, COSY, Heteronuclear Single Quantum Correlation (HSQC) and Heteronuclear Multiple Bond Correlation (HMBC). Chemical shifts were reported in parts per million (ppm), and coupling constants were expressed in Hz. Copies of ^{1}H and ^{13}C NMR spectra for all new compounds are given in the Supplementary Materials (Figures S1–S20). IR spectra were recorded by means of the KBr pellet technique on a Bruker Vector-22 spectrometer. UV spectra were obtained on an HP 8453 UV–Vis spectrometer (Hewlett-Packard, Waldbronn, Germany) in EtOH solution. Mass spectra were recorded with a Thermo Scientific DFS high-resolution mass spectrometer (Bremen, Germany) (evaporator temperature 200–250 °C, EI ionization at 70 V). Elemental analysis was carried out on a Carlo-Erba 1106-Elemental analysis instrument (Carlo-Erba, Milan, Italy).

The reaction progress and the purity of the obtained compounds were monitored by TLC on Silufol UV−254 plates (Kavalier, Czech Republic, $CHCl_3$/EtOH, 100:1; detection under UV light or by spraying the plates with a 10 % water solution of H_2SO_4 followed by heating at 100 °C). Column chromatography was performed with 60H silica gel (0.063–0.200 mm, Merck KGaA, Darmstadt, Germany). Propargyl bromide, coumarin-3-carboxylic acid **1**, DCC, DMAP and AcsNa were purchased from Alfa Aesar (GmbH, Karlsruhe, Germany). The starting materials: coumarin **4** [27,28], benzyl azide (**5a**) [29], aryl azides **5b**,**c**,**h** [30], azidobenzoic acid methyl ester isomers (**5d**–**f**) and 4-asidobensoic acid (**5g**) [31], *n*-butyl azide (**5i**) [32] and 1,5-diazidopentane (**6**) [33] were prepared following the literature procedures. The solvents (DMF, $CHCl_3$ and CH_2Cl_2) were purified according to the standard methods.

2.2. Synthesis

General Procedure for the Synthesis of Coumarino-1,2,3-triazolyl derivatives (**2a–i**)

To a stirred solution of alkynylcoumarin **4** (0.3 g, 1.3 mmol), substituted azide **5a–i** (1.1–1.5 mmol) or 1,5-diazidopentane (**6**) (0.6 mmol) in DMF (6 mL), copper sulfate $CuSO_4 \times 5H_2O$ (0.032 g, 0.13 mmol) and sodium ascorbate (0.026 g, 0.13 mmol) were added. The reaction mixture was kept under stirring at 75 °C for 6–8 h. After reaction completion, as indicated by TLC, the solvent was removed under reduced pressure, and the residue was treated with brine (30 mL) and extracted with EtOAc (3 × 30 mL). The organic layers were combined, washed with water (10 mL), dried over magnesium sulfate and filtered. The solvent was removed under reduced pressure, and the residue was subjected to column chromatography (chloroform-EtOH, 100:1→100:9). The initial coumarin (if conversion was incomplete) and reaction products are sequentially isolated. If necessary, the products are separated by repeated column chromatography to give compounds **2a–i** as white powders.

2.3. Characterization of Compounds *2a–i*

(1-Benzyl-1*H*-1,2,3-triazol-4-yl)methyl 2-oxo-2*H*-chromene-3-carboxylate (**2a**).

White powder (260 mg, 56%); mp 176–178 °C; IR (KBr, ν_{max}, cm^{-1}): 1757 (C=O), 1707 (C=O), 1618 (C=C), 1565 (C=N), 1494 (C=C), 1457 (C=C); UV (EtOH, λ_{max}, nm): 232, 295, 336; ^{1}H NMR (400 MHz, $CDCl_3$) δ 8.55 (s, 1H, H-4), 7.62 (m, 3H, H-5, 7, 12), 7.30 (m, 7H, H-6, 8, 15, 16, 17, 18, 19), 5.50 (s, 2H, H-10), 5.44 (s, 2H, H-13) ppm; ^{13}C NMR (125 MHz, $CDCl_3$) δ 162.3 (C-9), 156.4 (C-2), 155.1 (C-8a), 149.2 (C-7), 142.7 (C-11), 134.5 (C-5), 134.2 (C-14), 129.5 (C-17), 129.0 (C-16, 18), 128.7 (C-6), 128.1 (C-15, 19), 124.8 (C-12), 124.1 (C-4), 117.6 (C-4a), 117.2 (C-3), 116.7 (C-8), 58.7 (C-10), 54.1 (C-13) ppm; HRMS: found *m*/*z* 361.1054 $[M]^+$; calcd. for $C_{20}H_{15}N_3O_4$: M = 361.1057.

(1-Phenyl-1*H*-1,2,3-triazol-4-yl)methyl 2-oxo-2*H*-chromene-3-carboxylate (**2b**).White solid (290 mg, 65%); mp 139–141 °C; IR (KBr, ν_{max}, cm^{-1}): 1770 (C=O) 1705 (C=O), 1608 (C=C), 1563 C=N), 1504 (C=C), 1449 (C=C); UV (EtOH, λ_{max}, nm): 240, 295, 337; ^{1}H NMR (300 MHz, $CDCl_3$) δ 8.59 (s, 1H, H-4), 8.21 (s, 1H, H-12), 7.72 (d, *J* = 8.0 Hz, 2H, H-14, 18), 7.64 (t, *J* = 7.8 Hz, 1H, H-7), 7.58 (d, *J* = 7.8 Hz, 1H, H-5), 7.49 (t, *J* = 8.0 Hz, 2H, H-15, 17), 7.43 (d, *J* = 8.0 Hz, 1H, H-16), 7.33 (m, 2H, H-6, 8), 5.55 (s, 2H, H-10) ppm; ^{13}C NMR (125 MHz, $CDCl_3$) δ 162.3 (C-9), 156.5 (C-2), 155.0 (C-8a), 149.4 (C-7), 142.9 (C-11), 136.6 (C-13), 134.6 (C-5), 129.6 (C-14, 18), 128.8 (C-6), 124.8 (C-12), 122.5 (C-4), 120.4 (C-15, 17), 117.5 (C-4a), 116.9 (C-3), 116.7 (C-8), 58.6 (C-10) ppm; HRMS: found *m*/*z* 347.0901 $[M]^+$; calcd. for $C_{19}H_{13}N_3O_4$: M = 347.0903.

(1-(3,4-Dimethylphenyl)-1*H*-1,2,3-triazol-4-yl)methyl 2-oxo-2*H*-chromene-3-carboxylate (**2c**). White solid (430 mg, 88%); mp 133–135 °C; IR (KBr, ν_{max}, cm^{-1}): 1751 (C=O), 1707 (C=O), 1613 (C=C), 1564 (C=N), 1510 (C=C), 1454 (C=C); UV (EtOH, λ_{max}, nm): 257, 292, 337; ^{1}H NMR (500 MHz, $CDCl_3$) δ 8.60 (s, 1H, H-4), 8.16 (s, 1H, H-12), 7.65 (t, *J* = 7.8 Hz, 1H, H-7), 7.59 (d, *J* = 7.8 Hz, 1H, H-5), 7.50 (s, 1H, H-14), 7.41 (d, *J* = 8.1 Hz, 1H, H-18), 7.32 (m, 2H, H-6, 8), 7.23 (d, *J* = 8.1 Hz, 1H, H-17), 5.54 (s, 2H, H-10), 2.31 (s, 3H, H-20), 2.29 (s, 3H, H-19) ppm; ^{13}C NMR (125 MHz, $CDCl_3$) δ 162.3 (C-9), 156.5 (C-2), 155.1 (C-8a), 149.3 (C-7), 142.6 (C-11), 138.3 (C-15), 137.6 (C-16), 134.6 (C-5), 134.5 (C-13), 130.5 (C-18), 129.5 (C-6), 124.9 (C-17), 122.6 (C-4), 121.5 (C-12), 117.7 (C-14), 117.5 (C-14), 116.9 (C-3), 116.7 (C-8), 58.6 (C-10), 19.7 (C-20), 19.3 (C-19) ppm; HRMS: found *m*/*z* 375.1211 $[M]^+$; calcd. for $C_{21}H_{17}N_3O_4$: M = 375.1214.

(1-(2-(Methoxycarbonyl)phenyl)-1*H*-1,2,3-triazol-4-yl)methyl 2-oxo-2*H*-chromene- 3-carboxylate (**2d**). Brownish powder (350 mg, 67%); mp 114–117 °C; IR (KBr, ν_{max}, cm^{-1}): 1765 (C=O), 1725 (C=O), 1705 (C=O), 1609 (C=C), 1566 (C=N), 1498 (C=C), 1448 (C=C); UV (EtOH, λ_{max}, nm): 239, 293, 336; ^{1}H NMR (300 MHz, $CDCl_3$) δ 8.60 (s, 1H, H-4), 8.04 (s, 1H, H-12), 8.00 (d, *J* = 7.5 Hz, 1H, H-15), 7.60 (m, 4H, H-5, 7, 16, 17), 7.47(d, *J* = 7.8 Hz, 1H,

H-18), 7.33 (m, 2H, H-6, 8), 5.57 (s, 2H, H-10), 3.70 (s, 3H, OCH_3) ppm; ^{13}C NMR (75 MHz, $CDCl_3$) δ 165.0 (C-19), 162.0 (C-9), 156.1 (C-2), 154.8 (C-8a), 149.0 (C-7), 141.8 (C-11), 135.5 (C-14), 134.3 (C-5), 132.4 (C-15), 130.9 (C-17), 129.6 (C-18), 129.2 (C-16), 126.9 (C-13), 126.4 (C-6), 125.9 (C-4), 124.5 (C-12), 117.3 (C-4a), 116.8 (C-3), 116.4 (C-8), 58.5 (C-10), 52.3 (C-20) ppm; HRMS: found *m*/*z* 405.0957 $[M]^+$; calcd. for $C_{21}H_{15}N_3O_6$: M = 405.0955

(1-(3-(Methoxycarbonyl)phenyl)-1*H*-1,2,3-triazol-4-yl)methyl 2-oxo-2*H*-chromene- 3-carboxylate (**2e**). White powder (490 mg, 75%); mp 184–186 °C; IR (KBr, ν_{max}, cm^{-1}): 1753 (C=O), 1722 (C=O), 1703 (C=O), 1614 (C=C), 1563 (C=N), 1495 (C=C), 1447 (C=C); UV (EtOH, λ_{max}, nm): 240, 294, 337; ^1H NMR (400 MHz, $CDCl_3$) δ 8.60 (s, 1H, H-4), 8.35 (t, *J* = 1.8 Hz, 1H, H-14), 8.29 (s, 1H, H-12), 8.10 (dt, *J* = 7.8, 1.8 Hz, 1H, H-16), 8.01 (ddd, *J* = 8.0, 2.3, 1.2 Hz, 1H, H-18), 7.63 (m, 3H, H-5, 7, 17), 7.33 (m, 2H, H-6, 8), 5.56 (s, 2H, H-10), 3.95 (s, 3H, OCH_3) ppm; ^{13}C NMR (75 MHz, $CDCl_3$) δ 165.6 (C-19), 162.4 (C-9), 156.5 (C-2), 155.1 (C-8a), 149.5 (C-7), 143.3 (C-11), 136.9 (C-13), 134.7 (C-5), 132.2 (C-15), 130.0 (C-16), 129.8 (C-17), 129.6 (C-18), 124.9 (C-6), 124.7 (C-14), 122.5 (C-4), 121.1 (C-12), 117.6 (C-4a), 117.0 (C-3), 116.8 (C-8), 58.6 (C-10), 52.5 (C-20) ppm; HRMS: found *m*/*z* $[M]^+$ 405.0955; calcd. for $C_{21}H_{15}N_3O_6$: M = 405.0951.

(1-(4-(Methoxycarbonyl)phenyl)-1*H*-1,2,3-triazol-4-yl)methyl 2-oxo-2*H*-chromene- 3-carboxylate (**2f**). White powder (340 mg, 65%); mp 161–165 °C; IR (KBr, ν_{max}, cm^{-1}): 1771 (C=O), 1714 (C=O), 1705 (C=O), 1640 (C=C), 1611 (C=C), 1565 (C=N), 1520 (C=C), 1445 (C=C); UV (EtOH, λ_{max}, nm): 240, 281, 337; ^1H NMR (400 MHz, $CDCl_3$) δ 8.60 (s, 1H, H-4), 8.30 (s, 1H, H-12), 8.19 (d, *J* = 8.8 Hz, 2H, H-15, 17), 7.84 (d, *J* = 8.8 Hz, 2H, H-14, 18), 7.64 (t, *J* = 8.0 Hz, 1H, H-7), 7.59 (d, *J* = 8.0 Hz, 1H, H-5), 7.33 (m, 2H, H-6, 8), 5.56 (s, 2H, H-10), 3.93 (s, 3H, OCH_3) ppm; ^{13}C NMR (75 MHz, $CDCl_3$) δ 165.4 (C-19), 162.1 (C-9), 156.2 (C-2), 154.8 (C-8a), 149.2(C-7), 143.2 (C-11), 139.4 (C-13), 134.5 (C-5), 131.0 (C-15, 17), 130.1 (C-16), 129.4 (C-6), 124.7 (C-12), 122.0 (C-4), 119.6 (C-14, 18), 117.4 (C-4a), 116.6 (C-3), 116.5 (C-8), 58.3 (C-10), 52.1 (C-20) ppm; HRMS: found *m*/*z* 405.0952$[M]^+$; calcd. for $C_{21}H_{15}N_3O_6$: M = 405.0955.

4-(4-((2-Oxo-2*H*-chromene-3-carbonyloxy)methyl)-1*H*-1,2,3-triazol-1-yl)-benzoic acid (**2g**). White powder (460 mg, 90%); mp 260–262 °C (with decomp.); IR (KBr, ν_{max}, cm^{-1}): 3349 (OH), 1766 (C=O), 1716 (C=O), 1700 (C=O), 1640 (C=C), 1610 (C=C), 1565 (C=N), 1518 (C=C), 1445 (C=C); UV (EtOH, λ_{max}, nm): 235, 273, 337; ^1H NMR (400 MHz, DMSO-d_6) δ 9.05 (s, 1H, H-4), 8.81 (s, 1H, H-12), 8.11 (m, 4H, H-14,15,17,18), 7.93 (d, *J* = 7.4 Hz, 1H, H-5), 7.74 (t, *J* = 7.4 Hz, 1H, H-7), 7.42 (m, 2H, H-6,8), 5.50 (s, 2H, H-10) ppm; ^{13}C NMR (125 MHz, DMSO-d_6) δ 162.4(C-19), 162.1 (C-9), 155.9 (C-2), 154.7 (C-8a), 149.5(C-7), 143.2 (C-11), 139.4 (C-13), 134.9 (C-5), 131.4 (C-16), 130.5 (C-15, 17), 124.9 (C-14, 18), 123.5 (C-6), 120.2 (C-12), 117.9 (C-4), 116.9 (C-4a), 116.2 (C-3,8), 58.1 (C-10) ppm; HRMS: found *m*/*z* 391.0796 $[M]^+$; calcd. for $C_{20}H_{13}N_3O_6$: M = 391.0799.

(1-(4-Iodophenyl)-1*H*-1,2,3-triazol-4-yl)methyl 2-oxo-2*H*-chromene-3-carboxylate (**2h**). White powder (275 mg, 47%); mp 198–201 °C; IR (KBr, ν_{max}, cm^{-1}): 1739 (C=O), 1724 (C=O), 1612 (C=C), 1565 (C=N), 1495 (C=C), 1459 (C=C), 622 (C-I); UV (EtOH, λ_{max}, nm): 237, 265, 337; ^1H NMR (300 MHz, $CDCl_3$) δ ppm 8.58 (s, 1H, H-4), 8.20 (s, 1H, H-12), 7.83 (d, *J* = 8.6 Hz, 2H, H-15, 17), 7.67 (t, *J* = 7.8 Hz, 1H, H-7), 7.59 (d, *J* = 7.8 Hz, 1H, H-5), 7.49 (d, *J* = 8.6 Hz, 2H, H-14, 18), 7.33 (m, 2H, H-6, 8), 5.55 (s, 2H, H-10); ^{13}C NMR (75 MHz, $CDCl_3$) δ 162.5 (C-9), 156.5 (C-2), 155.2 (C-8a), 149.4 (C-7), 143.4 (C-11), 138.8 (C-15, 17), 136.4 (C-13), 134.7 (C-5), 129.6 (C-6), 124.9 (C-12), 122.3 (C-4), 122.0 (C-14, 18), 117.7 (C-4a), 117.2 (C-3), 116.8 (C-8), 93.8 (C-16), 58.7 (C-10) ppm; HRMS: found *m*/*z* 472.9966$[M]^+$; calcd. for $C_{19}H_{12}IN_3O_4$: M = 472.9867.

(1-Butyl-1*H*-1,2,3-triazol-4-yl)methyl 2-oxo-2*H*-chromene-3-carboxylate (**2i**). White powder (180 mg, 42%); mp 102–104 °C; IR (KBr, ν_{max}, cm^{-1}): 1774 (C=O), 1715 (C=O), 1648 (C=C), 1612 (C=C), 1566 (C=N), 1500 (C=C), 1453 (C=C); UV (EtOH, λ_{max}, nm): 238, 295,

335; ^{1}H NMR (300 MHz, $CDCl_3$) δ 8.60 (s, 1H, H-4), 7.75 (s, 1H, H-12), 7.63 (t, J = 7.8 Hz, 1H, H-7), 7.59 (d, J = 7.8 Hz, 1H, H-5), 7.32 (m, 2H, H-6, 8), 5.46 (s, 2H, H-10), 4.34 (t, J = 7.3 Hz, 2H, H-13), 1.87 (m, 2H, H-14), 1.33 (m, 2H, H-15), 0.93 (t, J = 7.0 Hz, 3H, H-16) ppm; ^{13}C NMR (125 MHz, $CDCl_3$) δ 162.3 (C-9), 156.6 (C-2), 155.1 (C-8a), 149.4 (C-7), 142.2 (C-11), 134.6 (C-5), 129.6 (C-6), 124.9 (C-12), 124.1 (C-4), 117.6 (C-4a), 117.0 (C-3), 116.7 (C-8), 58.7 (C-10), 50.0 (C-13), 32.1 (C-14), 19.6 (C-15), 13.3 (C-16) ppm; HRMS m/z found 327.1210 $[M]^+$; calcd. for $C_{17}H_{17}N_3O_4$: M = 327.1214.

Synthesis of (1,1′-(Pentane-1,5-diyl)*bis*(1H-1,2,3-triazole-4,1-diyl))*bis*(methylene) *bis*-(2-oxo-2*H*-chromene-3-carboxylate) (**3**)

To a stirred solution of alkynylcoumarin 4 (0.30 g, 1.3 mmol), 1,5-diazidopentane (6) (0.12 g, 0.66 mmol) in DMF (15 mL), copper sulfate $CuSO_4 \times 5H_2O$ (0.032 g, 0.13 mmol) and sodium ascorbate (0.026 g, 0.13 mmol) were added. The reaction mixture was kept under stirring at 75 °C for 12 h (TLC control). The solvent was removed under reduced pressure, and the residue was treated with brine (30 mL) and extracted with EtOAc (3 × 30 mL). The organic layers were combined, washed with water (10 mL), dried over magnesium sulfate and filtered. The solvent was removed under reduced pressure, and the residue was subjected to column chromatography (chloroform-EtOH, 100:1→100:9). Repeated column chromatography of the product fractions afforded compound 3 (260 mg, 66%). White powder; mp 171–173 °C; IR (KBr, ν_{max}, cm^{-1}): 1758 (C=O), 1709 (C=O), 1611 (C=C), 1565 (C=N), 1499 (C=C), 1453 (C=C); UV (EtOH, λ_{max}, nm): 239, 295, 336; ^{1}H NMR (300 MHz, $CDCl_3$) δ 8.57 (s, 2H, H-4, 4′), 7.75 (s, 2H, H-12, 12′), 7.61 (m, 4H, H-5, 5′, 7, 7′), 7.32 (m, 4H, H-6, 6′, 8, 8′), 5.44 (s, 4H, H-10, 20), 4.33 (m, 4H, H-13, 17), 1.94 (m, 4H, H-14, 16), 1.33 (m, 2H, H-15) ppm; ^{13}C NMR (75 MHz, $CDCl_3$) δ 162.3 (C-9, 21), 156.6 (C-2, 2′), 155.1 (C-8a, 8′a), 149.3 (C-7, 7′), 142.4 (C-11, 19), 134.6 (C-5, 5′), 129.7 (C-6, 6′), 124.9 (C-12, 18), 124.3 (C-4, 4′), 117.6 (C-4a, 4′a), 117.1 (C-3, 3′), 116.8 (C-8, 8′), 58.7 (C-10, 20), 49.8 (C-13, 17), 29.4 (C-14, 16), 23.3 (C-15) ppm; Found, %: C 59.55; H 4.60; N12.98. $C_{31}H_{26}N_6O_8 \times H_2O$. Calculated,%: C 59.23; H 4.45; N 13.17.

2.4. Biological Studies

2.4.1. Cell Culture and Cytotoxicity Assay

The HPV-negative human cervical cancer cell line C33 A, HPV16-positive human cervical cancer cell line CaSki, HPV18-positive human cervical cancer cell line HeLa, breast cancer (adenocarcinoma MCF-7) and prostate cancer (DU-145) were obtained from the American Type Culture Collection (ATCC). Normal epithelial VERO cells derived from the kidney of an African green monkey were used as a non-cancer control. This cell line was obtained from the cell collection of the State Research Center for Virology and Biotechnology "Vector" of Rospotrebnadzor, Koltsovo, Novosibirsk Region. The cells were cultured in DMEM/F12 medium containing 10% embryonic calf serum, L-glutamine (2 mmol/L) and gentamicin (80 μg/mL) in a CO_2 incubator at 37 °C. The tested compounds (**2a–i**, **3**) and a reference drug doxorubicin were dissolved in DMSO and added to the cellular culture at the required concentrations. Three wells were used for each concentration. The cells that were incubated without the compounds were used as controls. Cells were placed in 96-well microplates and cultivated at 37 °C in 5% CO_2/95% air for 48 h. The cell viability was assessed through a MTT [3-(4,5-dimethylthiazol-2-yl)-2,5-phenyl-2*H*-tetrazolium bromide] conversion assay [34], where 1% MTT was added to each well. Four hours later, the medium was removed, leaving the formazan crystals, and isopropanol was added and mixed for 15 min. The optical density of the samples was measured on a Thermo Multiskan FC spectrophotometer (Thermo Fisher Scientific, USA) at a wavelength of 540 nm, with a reference of 670 nm. The 50% cytotoxic dose (GI_{50}) of each compound (i.e., the compound concentration that lowers the amount of cells to 50% in a culture or decreases the optical

density twofold as compared to the control wells) was calculated from the obtained data. All data are presented as the mean ± SEM from at least three independent experiments. Statistical analysis of the results was performed using the Microsoft Excel 2007, STATISTICA 6.0 and GraphPad Prism 5.0 programs, and significance was defined as $p < 0.05$ (*t*-test). The results are given as the average value ± standard deviation from the average.

2.4.2. Cell Cycle Analysis

For the cell cycle analysis, cells were seeded in 6-well plates (3×10^5 per plate) and incubated for adhesion for 24 h. After that, cells were washed twice in an ice-cold PBS buffer and treated with the tested compounds dissolved in DMSO in GI_{50} concentration, then incubated for 24 and 48 h. Control wells received only 0.1% DMSO. Cells were washed with PBS twice, harvested, pelleted and resuspended in 0.5 mL of PBS. For staining, the propidium iodide (PI, Sigma-Aldrich) was used according to the instructions. A BD FACSCanto™ II flow cytometer (Becton Dickinson FACScan, Sunnyvale, CA, USA) equipped with CellQuest 3.2 software (Becton Dickinson) was used to analyze the cell cycle phase distribution. The results were presented as a percentage of cell population standing in different stages of the cell cycle. To perform statistical analyses, pairwise comparisons were made between untreated and treated cells at the same stage of the cell cycle. For example, growth inhibition after treatment with doxorubicin or a test compound was compared to the growth inhibition of untreated cells. At least 3×10^5 cells acquired for each sample were recorded and analyzed.

2.4.3. Cell Death by Annexin V-FITC/PI Staining Analyzed by Flow Cytometry

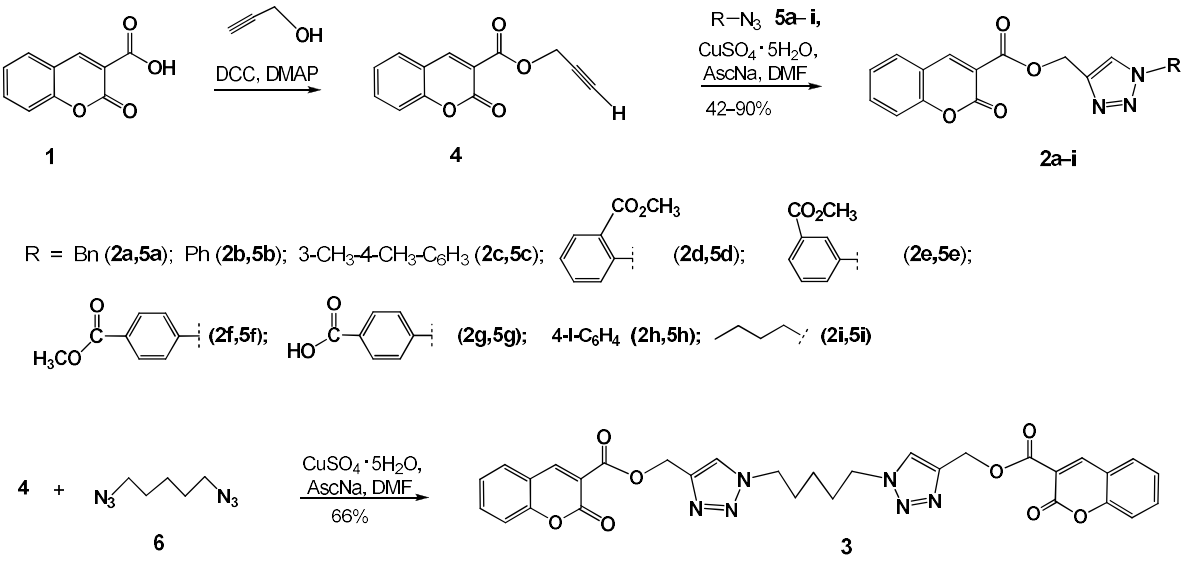
The Annexin V-FITC and PI apoptosis assay kits were used to distinguish early and late stage apoptotic cell death from necrosis by the standard FACS assay. The C33 A and CaSki cells (3×10^5 cell/mL) were seeded in a 24-well plate and incubated for 24 h. The compounds at a concentration of $1 \times GI_{50}$ (4.4 μM for **2g** or 7.0 μM for **3**) were added and incubated for 12 and 24 h. After that, the cells were washed with PBS twice. The cells were then resuspended with 95 mL of binding buffer, followed by staining with 100 mL of Annexin V-FITC (5 mL in 95 mL of buffer) for 15 min (dark condition). Then, the cells were stained with 100 mL of PI solution (5 μL of PI in 95 μL of binding buffer) and incubated for another 15 min in the dark at RT. The cells were analyzed by flow cytometry (BD FACSCanto™ II, BD Biosciences, San Jose, CA, USA). The percentage viable, apoptotic and necrotic cells were detected by BD FACSDiva Software 6.0 (BD Biosciences, San Jose, CA, USA). Data analysis was performed using BD FACSDiva software (BD Biosciences, San Jose, CA, USA).

3. Results

3.1. Chemistry

Scheme 1 shows a brief description of the route used for the synthesis of new 3-substituted coumarin derivatives **2a**–**i** and **3**. The key alkyne coumarin **4** was synthesized in a quantitative yield by the propargylation of coumarin-3-carboxylic acid **1** with propargyl alcohol according to reported methods [27,28]. 3-Alkynyl substituted coumarin **4** was obtained in excellent yield and was pure enough for further reactions. Next, the Cu(I)-catalyzed alkyne-azide 1,3-dipolar cycloaddition (CuAAC reaction) was used for the synthesis of 3-triazolyl-methoxycarbonyl-substituted coumarins **2a**–**i** and **3**. We have chosen the most simple and well-characterized variant, namely, carrying out the reaction in DMF, with catalysis of the Cu(I) ions generated in situ from $CuSO_4$ and sodium ascorbate [35–37]. CuAAC reaction of ethynyl coumarin **4** with azides, namely, benzyl azide **5a**, phenyl azide **5b**, 4-azido-1,2-dimethylbenzene **5c**, three positional azidobenzoic acid

methyl ester isomers **5d**–**f**, 4-azidobensoic acid **5g**, 1-azido-4-iodobenzene **5h** or *n*-butyl azide **5i**, afforded the 1-benzyl-, 1-aryl- or 1-butyl-substituted (1,2,3-triazol-4-yl)methyl 2-oxo-2*H*-chromene-3-carboxylates (**2a**–**i**) in 42–90% yields (Scheme 1). The higher yield (88–90%) was observed in the reaction of 4 with aryl azides **5b**,**g**.



Scheme 1. Synthesis of coumarino-1,2,3-triazolyl derivatives **2a**–**i** and **3**. DCC = N,N′- dicyclohexyl-carbodiimide; DMAP = 4-dimethylaminopyridine; AscNa = sodium ascorbate.

It is known that functionalized *bis*-coumarins are often shown to be more effective against cancer cell lines than the monomeric species [38–40]. We successfully employed the CuAAC reaction of 3-alkynyl-substituted coumarin **4** with diazide for the synthesis of the *bis*(coumarino-3carboxylate)-*bis*(triazolyl) compound. The reaction of compound **4** with 1,5-diazidopentane **6** (0.51 equiv.) under higher dilution conditions by using the simple copper(II) sulfate and sodium ascorbate system to generate the cooper(I) catalyst proceeded with the formation of (pentane-1,5-diyl-*bis*(1*H*-1,2,3-triazole-1,4-diyl))*bis*(methylene) *bis*(2-oxo-2*H*-chromene-3-carboxylate) **3** isolated in the yield 66% after column chromatography on silica gel (Scheme 1).

The composition and structure of the synthesized compounds were confirmed by IR, ^{1}H and ^{13}C NMR spectroscopy; mass spectrometry and elemental analysis data. The ^{1}H and ^{13}C NMR spectra of the obtained compounds contained one set of signals characteristic for the coumarin backbone and the corresponding substituent. Formation of the 1,2,3-triazole ring in compounds **2a**–**i** and **3** was confirmed by the NMR data. The ^{1}H NMR spectra exhibited singlet signals for the H-triazole proton (δ 7.75–8.30 ppm). The ^{13}C NMR signals of the C-4 and C-5 triazole carbon atoms were observed in the regions of δ = 136.6–142.2 ppm and δ = 120.8–124.9 ppm, respectively. These data confirm the regioselectivity of the studied copper-catalyzed azide-alkyne cycloaddition, giving 1,4-disubstituted 1,2,3-triazoles **2a**–**i** or (pentane-1,5-diyl-*bis* (1*H*-1,2,3-triazole-1,4-diyl))- *bis*(methylene) *bis*(2-oxo-2*H*-chromene-3-carboxylate) **3** [41].

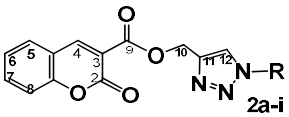
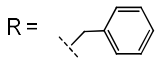
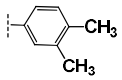
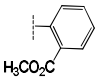
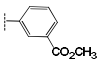
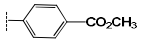
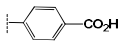
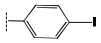
3.2. Biological Study

3.2.1. Cytotoxicity Assay

All new compounds **2a**–**i** and **3** were screened for their in vitro cytotoxicity and growth inhibitory activities against three different tumor types, namely, the HPV-negative human cervical cancer cell line C33 A, HPV16-positive human cervical cancer cell line CaSki, HPV18-positive human cervical cancer cell line HeLa, breast cancer (adenocarcinoma MCF-7) and prostate cancer DU-145 cell lines, in comparison with the activity of the known

anticancer reference drug doxorubicin (DOX). Normal epithelial VERO cells were used as a non-cancer control. Cell viability was assessed by the 3-[4,5-dimethyl-thiazol-2-yl]- 2,5-diphenyltetrazolium bromide (MTT) assay. The cytotoxic activities of the tested compounds were expressed as the GI_{50} μM value (the dose that reduces growth inhibition to 50%) (Table 1). All tested triazole–coumarin derivatives **2a–i** and **3** were nontoxic for VERO cells (GI_{50} >100 μM) relative to doxorubicin (GI_{50} = 8 ± 1.8 μM) (Table 1). The substituent at position N1 in the triazole ring can enhance bioactivity, and differential bioactivity exhibited by coumarin might be associated with its substitution position. Compounds with the N1 aryl-substituted triazolyl–coumarin esters **2d–h** exhibited selective cytotoxicity towards cervical cancer cell lines C33 A.

Table 1. Concentrations of half-maximal inhibition (GI_{50} ± SEM, μM) on five cancer cell lines and VERO cells for compounds **2a–i** and **3**.

Compound		Growth Inhibition of Cells (GI_{50} ± SEM, μM) [a, b]					
 2a-i		C33 A (HPV-Negative)	CaSki (HPV-16)	HeLa (HPV-18)	MCF-7	DU-145	VERO
2a	R = 	>100	56 ± 3.6	29 ± 2.0	51 ± 2.9	>100	>100
2b		81 ± 0.2	38 ± 3.2	35 ± 4.0	41 ± 2.1	>100	>100
2c		76 ± 4.1	33 ± 1.5	29 ± 1.8	62 ± 1.5	>100	>100
2d		21 ± 1.7	19 ± 0.9	27 ± 1.7	40 ± 2.7	34 ± 2.0	>100
2e		31 ± 3.1	25 ± 1.4	32 ± 2.5	36 ± 1.1	41 ± 2.9	>100
2f		25 ± 1.1	22 ± 1.8	23 ± 0.9	30 ± 1.7	48 ± 1.6	>100
2g		4.4 ± 0.5	18 ± 2.5	22 ± 1.4	24 ± 1.6	19 ± 1.0	>100
2h		17 ± 1.1	20 ± 0.2	18 ± 1.3	31 ± 0.9	35 ± 1.1	>100
2i	$R = C_4H_9$	36 ± 2.5	31 ± 1.6	29 ± 1.1	34 ± 1.5	56 ± 3.6	>100
3		7.0 ± 2.6	15 ± 1.6	20 ± 1.2	25 ± 2.0	22 ± 1.2	>100
Doxorubicin		2.5 ± 0.8	10.1 ± 0.7	6.1 ± 0.7	5.2 ± 0.8	15 ± 0.3	8 ± 1.8

[a] GI_{50}: concentration at which 50% growth inhibition of tumor cells is observed after 48 h incubation. [b] The experimental results are given as the data average values obtained from three independently conducted experiments.

3.2.2. Cell Cycle Analysis

At the next stage, we performed the cell cycle analysis in cervical cancer cell lines C33 A (Table 2 and Figure 2) and CaSki (Table 3 and Figure 3). For the analysis, only intact cells were selected. At least 3×10^5 cells were acquired per each sample. Non-treated cells in DMSO were taken as a control place.

Compound **3** suppressed cell proliferation in C33 A cells at a relatively low concentration (7.0 μM). Examining the data for compound **2g** showed that a good number of cells were distributed in the G1 phase, i.e., in the growth phase on the cell cycle. In contrast, compound **3** induced a significant block of cells in the G2 phase after 24 h, while the proportion of cells in the growth phases was reduced after 48 h of incubation (Table 2 and Figure 2). Compound **3** initiated the subG1 phase: 80.9% apoptotic and necrosis cells were formed after 48 h of incubation. In contrast, cell cycle analysis in cervical cancer cell

line C33 A for doxorubicin (DOX) (GI_{50} concentration) showed 20.5% cell death after 48 h of incubation.

Table 2. Cell cycle analysis in cervical cancer cell line C33 A.

Compound	Concentration, μM	Population (% Cell Distribution) [b]							
		24 h				48 h			
		G1	S	G2	SubG1	G1	S	G2	SubG1
2g	4.4 (GI_{50})	55.9	16.7	24.1	3.3	50.5	16.5	27.2	5.8
3	7.0 (GI_{50})	21.8	15.9	49.9	12.3	4.2	5.5	9.4	80.9
DOX	2.5 (GI_{50})	8.3	21.5	67.7	2.5	9.4	24.3	45.8	20.5
Control + DMSO [a]		57.6	19.3	20.7	2.4	61.4	18.8	17.7	2.1
Control [a]		59.3	14.7	24.2	1.8	61.7	17.5	18.4	2.4

[a] Non-treated cells. [b] The results are presented as a percentage of the cell population standing in different stages of the cell cycle. All results obtained for the tested compounds are significantly different from the control (the comparison was made with untreated cells).

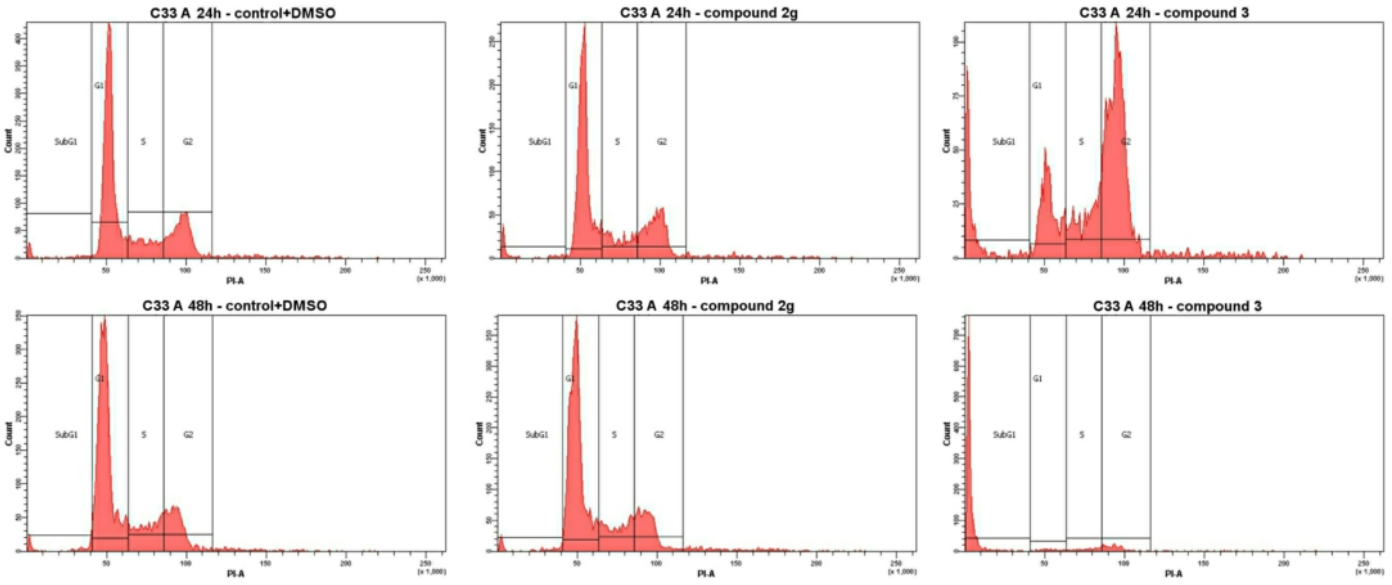


Figure 2. Effects of compounds **2g** and **3** on the cell cycle phase distribution in C33 A cells after treatment with the GI_{50} concentration during 24 and 48 h by using propidium iodide to determine the DNA fluorescence.

Since compounds **2g** and **3** showed their potential to reduce the cell viability of cervical cancer cells, we further investigated whether this effect is due to programmed cell death or necrosis. C33 A cells were treated with a 4.4 μM concentration of **2g** or 7.0 μM of **3** for 12 and 24 h (Figure 4). The induction of apoptosis was measured by Annexin V-FITC/PI staining. The flow cytometry data, as shown in Figure 4, depicted the increase in the event of apoptosis of the treated cells, especially for compound **3** compared to the control (DMSO-treated). The early apoptotic cell population increased to ~23% (early apoptosis) and ~6% (late apoptosis), respectively.

Table 3. Cell cycle analysis in cervical cancer cell line CaSki.

Compound	Concentration, μM	Population (% Cell Distribution) [b]							
		24 h				48 h			
		G1	S	G2	SubG1	G1	S	G2	SubG1
2g	18.0 (GI_{50})	46.7	19.4	29.8	4.1	43.7	16.7	28.3	11.3
3	15.0 (GI_{50})	42.5	19.9	28.5	9.1	42.4	17.9	29.7	10.0
DOX	10.1 (GI_{50})	24.8	5.6	5.8	63.8	24.6	8.0	4.7	62.7
Control + DMSO [a]		60.3	17.7	19.6	1.4	59.7	15.7	19.1	2.2
Control [a]		61.8	16.0	21.0	1.2	61.1	17.6	19.5	1.8

[a] Non-treated cells. [b] The results are presented as a percentage of the cell population standing in different stages of the cell cycle. All results obtained for the tested compounds are significantly different from the control (the comparison was made with untreated cells).

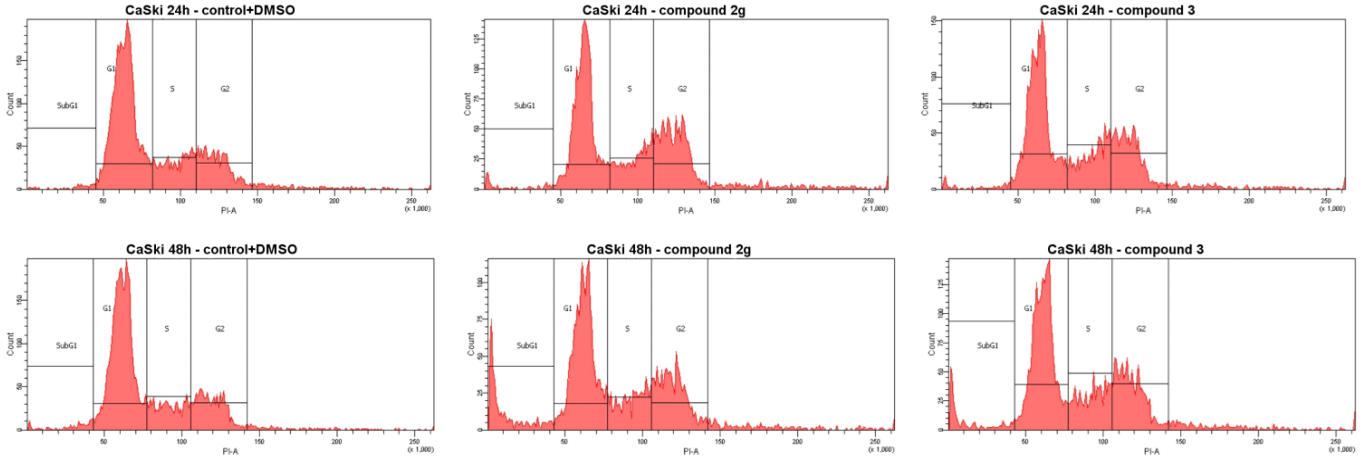


Figure 3. Effects of compounds **2g** and **3** on the cell cycle phase distribution in CaSki cells after treatment with the GI_{50} concentration during 24 and 48 h by using propidium iodide to determine the DNA fluorescence. Compounds are significantly different from the control (the comparison was made with untreated cells).

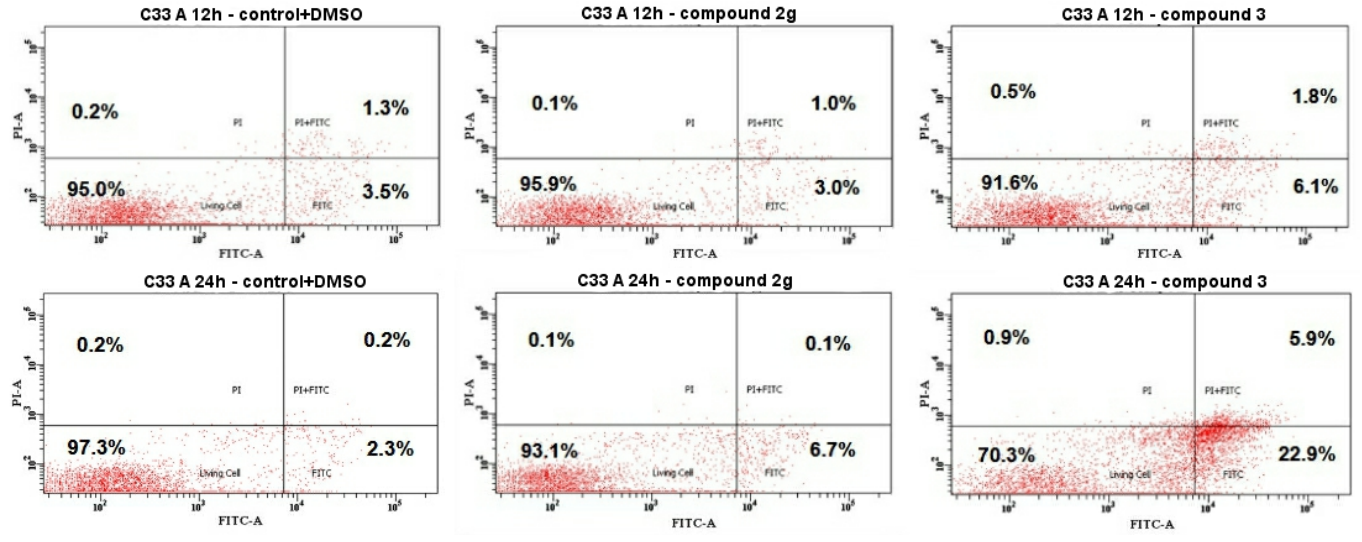


Figure 4. Flow cytometry histograms of the C33 A cells after being treated with compounds **2g** and **3** and the untreated C33 A cells (control+DMSO). Cells were treated at GI_{50} concentrations for 12 and 24 h.

Figure 5 listed the flow cytometry data for CaSki cells treated with compounds **2g** and **3** with the GI_{50} concentration. A time-dependent increase of apoptosis was shown for both compounds. The treatment with compound **2g** caused the greatest effect. The early apoptosis cell population increased from 19% after 12 h of treatment to 51.4% after 24 h of treatment. The late apoptosis population cells also increased from 3.8 (12 h) to 9.1% (24 h). The number of cells in the necrotic stage amounted to only 0.1%. Meanwhile, flow cytometry analysis proved that compound **3** was also time-dependent and obviously increased the percentage of apoptotic cells, from 6.1 and 1.8% for 12 h to 22.9 and 5.9% for 24 h (compared to the control (DMSO-treated).

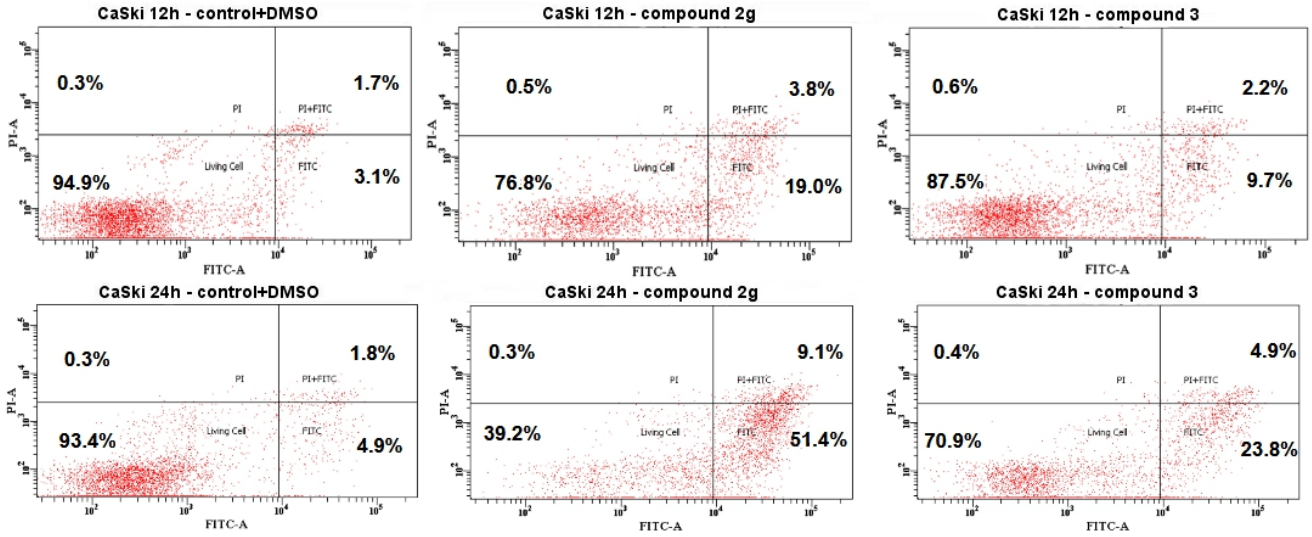


Figure 5. Flow cytometry histograms of the CaSki cells after being treated with compounds **2g** and **3** and the untreated CaSki cells (C+DMSO). Cells were treated at the GI_{50} concentrations for 12 and 24 h.

4. Discussion

Currently, we are studying the synthesis and cytotoxicity of compounds with coumarin-3-carboxylate and triazole pharmacophores. The SAR revealed that the substituent at the N1 position of the triazole ring has a great influence on the cytotoxicity. Compounds **2a**–**c** with benzyl, phenyl and 3,4-dimethylphenyl substituents exhibited low or insignificant cytotoxicity with high GI_{50} values on the MCF-7 and DU-145 cancer cell lines and showed much more potent cytotoxicity with significantly lower GI_{50} values on the HeLa tumor cells. Spacing the aromatic ring with a methoxycarbonyl substituent (compounds **2d**,**e**,**f**) greatly increased the cytotoxicity, especially in relation to cervical cancer cells C33 A and CaSki. The cytotoxicity was greatly dependent on the C-2, C-3 and C-4 substitution positions in the phenyl ring attached to the N1 position of the 1,2,3-triazole moiety in the coumarin–triazolyl ester conjugates. Modification of the N1 position of the triazole ring with a 4-carboxyphenyl or 4-iodophenyl substituent (compounds **2g**,**h**) can significantly potentiate the anticancer activity on the cervical cancer cell lines. The great dependence of cytotoxicity on the substituents that are present at the C-2, C-3 and C-4 positions of the phenyl ring that are directly attached to the 1,2,3-triazole moiety in coumarin-tethered bis-triazoles was shown previously [42].

Comparatively reduced cytotoxicity was found for the linear 1-*n*-butyl-substituted (monomeric) coumarin–triazolyl ester conjugate **2i**. Overall, compounds **2g** and **3** exhibited general cytotoxicity on various forms of cervical cancer cells and possessed the highest degree of cytotoxicity towards the HPV-negative human cervical cancer cells C33 A (GI_{50} 4.4 ± 1.3 and 7.0 ± 2.6 μM, respectively) (Table 1).

Substituted coumarins can show anticancer activity through diverse mechanisms. These include inhibiting the expression or action of enzymes such as topoisomerase, human carbonic anhydrase and telomerase, causing cell apoptosis, estrogen receptor modification or cell cycle arrest at different phases [43,44]. The cell cycle analysis in cervical cancer cell lines C33 A (Table 2 and Figure 2) and CaSki (Table 3 and Figure 3) produced interesting results.

Compounds **2g** and **3** suppress cell proliferation in C33 A cells at a relatively low concentration (4.4 and 7.0 μM). Examining the data for compound **2g**, showed that a good number of cells was distributed in the G1 phase, i.e., in the growth phases of the cell cycle. In contrast, compound **3** induced a significant block of cells in the G2 phase after 24 h, while the proportion of cells in the growth phases was reduced after 48 h of incubation (Table 2 and Figure 2). Compound **3** at a 1 × GI_{50} concentration initiated the subG1 phase: 80.9% apoptotic and necrosis cells were formed after 48 h of incubation. In contrast, cell cycle analysis in cervical cancer cell line C33 A for doxorubicin (GI_{50} concentration, 7.0 μM) showed 20.5% cell death after 48 h of incubation.

No significant difference in the actions of compound **2g** and **3** on the cell cycle was observed during the progression of the cell cycle in CaSki cells. All the treated tumor cells showed significant morphological changes such as cell shrinkage, detachment and membrane blebbing. The most pronounced effect was found for compound **2g**: an increase in the population of CaSki cells in the SubG1 phase to 11.3% was observed after 48 h of treatment by decreasing the number of cells in the G1 phases. Compound **3** increased the number of cells in the S/G2 phase compared to normal cancer cells and induced cell cycle arrest in the S/G2 phase. In contrast, doxorubicin initiated the subG1 phase after 24 and also 48 h to almost 63% (Table 3 and Figure 3). Our result suggests that compounds **2g** and **3** in the GI_{50} concentration in CaSki cells induced cell cycle arrest in the S/G2 phase, which seems to be partly responsible for the inhibition of cell proliferation.

Apoptosis and necrosis are among several forms of cell death mechanisms that are involved in the elimination of cancer cells, leading to successful therapy [45,46]. Loss of apoptosis is commonly found in most of the drug-resistant cancers [47]. Therefore, the induction of apoptosis in the target cancer cells is the therapeutic goal for any cancer therapy. In contrast, necrosis can trigger an inflammatory response that is not efficiently cleared by macrophages [48].

Tumor cell death, triggered by the most active bis-coumarin **3** on the HPV-negative human cervical cancer cells C33 A, resulted from apoptotic processes (Figure 4). At 24 h and the GI_{50} concentration (7.0 μM), compound **3** induced C33 A apoptotic cell death (22.9% early stage of apoptosis and 5.9% late stage of apoptosis). Interestingly, *bis*-coumarin **3** at the GI_{50} concentration caused a low necrosis percentage (0.9%)

The data in Figure 5 indicated that both compounds **2g** and **3** induced early apoptosis in the CaSki cell line. At 24 h, compound **2** induced the greatest apoptosis percentage at the GI_{50} concentration (51.4% of early stage and 9.1% of late stage apoptosis, respectively) with low necrotic cell death (0.3%). The apoptosis induced by compound **2** at the GI_{50} concentration was higher when compared to bis-coumarin **3** (23.8% of the early stage and 4.9% of late stage apoptosis, respectively).

Overall, in the present study, we first observed that N1-substituted 3-(1,2,3-triazolylmethoxycarbonyl)coumarins 2d-h and, especially, *bis*(coumarine-3-carboxylate)*bis*(1,2,3-triazole)pentan-1,5-diyl 3 possessed cell growth inhibition activity on cervical cancer cell lines, especially on the HPV-negative human cancer cells C33 A, exhibited bioactivity to induce apoptosis in cervical cancer cells C33 A and CaSki and were nontoxic to normal epithelial cells VERO. Notably, C33 A cells are negative for both DNA and RNA of human papillomavirus (HPV), distinguishing them from many other cervical cancer cell lines that

often carry HPV integrations—in particular, CaSki and HeLa. This aspect makes the new compounds particularly valuable for studying cervical cancer that develops independently of HPV infection, including insights into alternative pathways of carcinogenesis.

5. Conclusions

Here, we describe a mild and convenient method for the preparation of 3-(triazolylmeth oxycarbonyl)-substituted coumarins and (pentane-1,5-diyl-*bis*(1*H*-1,2,3-triazole-1,4-diyl))*bis* (methylene) *bis*(2-oxo-2*H*-chromene-3- carboxylate). The copper catalyzed cycloaddition of 3-propynyl substituted 2-oxo-2*H*-chromene-3-carboxylate with several azides, and diazide was the main synthetic method. The new series of 1,2,3-triazolyl-modified coumarins was evaluated for their in vitro anticancer activity against human cancer cell lines using the conventional MTT assay. All compounds were nontoxic towards normal epithelial VERO cells. Among all 3-(1,2,3-triazolylmethoxycarbonyl)coumarins synthesized, coumarin derivatives with a 4-carboxyphenyl substituent at the N1-position of the triazole ring **2g** exhibited better activity in the series on cervical cancer cells (C33 A, CaSki and HeLa); breast carcinoma cells MCF-7 and prostate cancer cells DU-145. The *bis*(coumarino-1,2,3-triazol) with pentamethylene linker **3** possessed the most promising cytotoxic potential towards cervical cancer cells (C33 A and CaSki). These results validate the potential of 3-(1,2,3-triazolylmethoxycarbonyl)-substituted coumarins used as anticancer agents, particularly against cervical cancer, and provide important, potentially helpful steps in drug designing and discovery.

Supplementary Materials: The following supporting information can be downloaded at https://www.mdpi.com/article/10.3390/scipharm93020016/s1: Copies of ^{1}H and ^{13}C NMR spectra for all new compounds.

Author Contributions: Conceptualization: A.S.K. and E.E.S.; methodology: M.S.H., M.A.P., Z.R.S., A.S.A., G.K.M. and V.A.S.; software: E.E.S. and A.G.P.; validation, A.S.K. and A.G.P.; formal analysis: A.S.K., M.S.H. and V.A.S.; investigation: A.S.K., M.S.H., M.A.P., Z.R.S., A.S.A. and G.K.M.; resources: A.S.K., E.E.S. and A.G.P.; data curation, E.E.S. and A.G.P.; writing—original draft preparation: A.S.K., M.S.H. and V.A.S.; writing—review and editing: A.S.K., M.S.H. and E.E.S.; visualization, A.G.P.; supervision, A.S.K.; project administration: A.S.K.; funding acquisition: A.S.K. All authors have read and agreed to the published version of the manuscript.

Funding: This research was funded by the Ministry of Science and Education of the Republic of Kazakhstan (grant number: AP 19579011).

Institutional Review Board Statement: Not applicable.

Informed Consent Statement: Not applicable.

Data Availability Statement: Samples of the synthesized compounds are available from the authors.

Acknowledgments: The authors would like to acknowledge the Multi-Access Chemical Research Center SB RAS for spectral and analytical measurements.

Conflicts of Interest: The authors declare no conflicts of interest. The funders had no role in the design of the study; in the collection, analyses or interpretation of the data; in the writing of the manuscript or in the decision to publish the results.

References

1. Salem, M.A.; Marzouk, M.I.; El-Kazak, A.M. Synthesis and characterization of some new coumarins with in vitro antitumor and antioxidant activity and high protective effects against DNA damage. *Molecules* **2016**, *21*, 249–269. [CrossRef] [PubMed]
2. Majhi, A.; Venkateswarlu, K.; Sasikumar, P. Coumarin based fluorescent probe for detecting heavy metal ions. *J. Fluoresc.* **2024**, *34*, 1453–1483. [CrossRef]

3. Sokol, I.; Toma, M.; Krnić, M.; Macan, A.M.; Drenjančević, D.; Liekens, S.; Raić-Malić, S.; Gazivoda Kraljević, T. Transition metal-catalyzed synthesis of new 3-substituted coumarin derivatives as antibacterial and cytostatic agents. *Future Med. Chem.* **2021**, *13*, 1865–1884. [CrossRef]
4. Ghouse, S.M.; Bahatam, K.; Angeli, A.; Pawar, G.; Chinchilli, K.K.; Yaddanapudi, V.M.; Mohammed, A.; Supuran, C.T.; Nanduri, S. Synthesis and biological evaluation of new 3-substituted coumarin derivatives as selective inhibitors of human carbonic anhydrase IX and XII. *J. Enzym. Inhib. Med. Chem.* **2023**, *38*, 2185760. [CrossRef]
5. Gao, L.; Wang, F.; Chen, Y.; Li, F.; Han, B.; Liu, D. The antithrombotic activity of natural and synthetic coumarins. *Fitoterapia* **2021**, *154*, 104947. [CrossRef]
6. Ramsis, T.M.; Ebrahim, M.A.; Fayed, E.A. Synthetic coumarin derivatives with anticoagulation and antiplatelet aggregation inhibitory effects. *Med. Chem. Res.* **2023**, *32*, 2269–2278. [CrossRef]
7. Tan, X.; Soualmia, F.; Furio, L.; Renard, J.-F.; Kempen, I.; Qin, L.; Pagano, M.; Pirotte, B.; El Amri, C.; Hovnanian, A.; et al. Toward the first class of suicide inhibitors of kallikreins involved in skin diseases. *J. Med. Chem.* **2015**, *58*, 598–612. [CrossRef]
8. Hanke, S.; Tindall, C.A.; Pippel, J.; Ulbricht, D.; Pirotte, B.; Reboud-Ravaux, M.; Heiker, J.T.; Sträter, N. Structural studies on the inhibitory binding mode of aromatic coumarinic esters to human kallikrein-related peptidase 7. *J. Med. Chem.* **2020**, *63*, 5723–5733. [CrossRef]
9. Frédérick, R.; Robert, S.; Charlier, C.; Wouters, J.; Masereel, B.; Pochet, L. Mechanism-based thrombin inhibitors: Design, synthesis, and molecular docking of a new selective 2-oxo-2*H*-1-benzopyran derivative. *J. Med. Chem.* **2007**, *50*, 3645–3650. [CrossRef]
10. Davoine, C.; Traina, A.; Evrard, J.; Lanners, S.; Fillet, M.; Pochet, L. Coumarins as factor XIIa inhibitors: Potency and selectivity improvements using a fragment-based strategy. *Eur. J. Med. Chem.* **2023**, *259*, 115636. [CrossRef]
11. Liu, H.; Xia, D.G.; Chu, Z.W.; Hu, R.; Cheng, X.; Lv, X.H. Novel coumarin-thiazolyl ester derivatives as potential DNA gyrase Inhibitors: Design, synthesis, and antibacterial activity. *Bioorg. Chem.* **2020**, *100*, 103907. [CrossRef] [PubMed]
12. Nelson, G.L.; Ronayne, C.T.; Solano, L.N.; Jonnalagadda, S.K.; Jonnalagadda, S.; Schumacher, T.J.; Gardner, Z.S.; Palle, H.; Mani, C.; Rumbley, J.; et al. Synthesis and biological evaluation of N, N-dialkylcarboxy coumarin-NO donor conjugates as potential anticancer agents. *Bioorg. Med. Chem. Lett.* **2021**, *52*, 128411. [CrossRef] [PubMed]
13. He, B.; Ding, L.; Tan, H.; Liu, C.-B.; He, L.-Q. Synthesis and antitumor activity evaluation of coumarin Mannich base derivatives. *Chem. Biol. Drug Des.* **2024**, *103*, e14389. [CrossRef]
14. Jain, A.; Piplani, P. Exploring the chemistry and therapeutic potential of triazoles: A comprehensive literature. *Mini Rev. Med. Chem.* **2019**, *19*, 1298–1368.
15. Guo, H.-Y.; Chen, Z.A.; Shen, Q.-K.; Quan, Z.-S. Application of triazoles in the structural modification of natural products. *J. Enzyme Inhib. Med. Chem.* **2021**, *36*, 1115–1144. [CrossRef]
16. Alam, M.M. 1,2,3-Triazole hybrids as anticancer agents: A review. *Arch. Pharm.* **2022**, *355*, e2100158. [CrossRef]
17. Rohman, N.; Ardiansah, B.; Wukirsari, T.; Judeh, Z. Recent trends in the synthesis and bioactivity of coumarin, coumarin-chalcone, and coumarin-triazole molecular hybrids. *Molecules* **2024**, *29*, 1026. [CrossRef]
18. Pršir, K.; Horak, E.; Kralj, M.; Uzelac, L.; Liekens, S.; Steinberg, I.M.; Krištafor, S. Design, synthesis, spectroscopic characterisation and in vitro cytostatic evaluation of novel bis(coumarin-1,2,3-triazolyl)benzenes and hybrid coumarin-1,2,3-triazolyl-aryl derivatives. *Molecules* **2022**, *27*, 637. [CrossRef]
19. Maiti, S.; Park, N.; Han, J.H.; Jeon, H.M.; Lee, J.H.; Bhuniya, S.; Kang, C.; Kim, J.S. Gemcitabine–coumarin–biotin conjugates: A target specific theranostic anticancer prodrug. *J. Am. Chem. Soc.* **2013**, *135*, 4567–4572. [CrossRef]
20. Fan, Y.L.; Ke, X.; Liu, M. Coumarin–triazole hybrids and their biological activities. *J. Heterocycl. Chem.* **2018**, *55*, 791–802. [CrossRef]
21. Slanova, K.; Todorov, L.; Belskaya, N.P.; Palafox, M.A.; Kostova, I.P. Developments in the application of 1,2,3-triazoles in cancer treatment. *Recent Pat. Anti-Cancer Drug Discov.* **2020**, *15*, 92–112. [CrossRef] [PubMed]
22. López, S.; Gracia, I.; Plaza-Pedroche, R.; Rodríguez, J.F.; Pérez-Ortiz, J.M.; Rodríguez-López, J.; Ramos, M.J. *In vitro* antioxidant and pancreatic anticancer activity of novel 5-fluorouracil-coumarin conjugates. *Pharmaceutics* **2022**, *14*, 2152. [CrossRef] [PubMed]
23. Nesaragi, A.R.; Algethami, J.S.; Alsaiari, M.; Alsareii, S.A.; Mathada, B.S.; Ningaiah, S.; Sasidhar, B.S.; Harraz, F.A.; Patil, S.A. A comprehensive overview of coumarinyl-triazole hybrids as anticancer agents. *J. Mol. Struct.* **2024**, *1302*, 137478. [CrossRef]
24. Lipeeva, A.V.; Zakharov, D.O.; Burova, L.G.; Frolova, T.S.; Baev, D.S.; Shirokikh, I.V.; Evstropov, A.N.; Sinitsyna, O.I.; Tolstikova, T.G.; Shults, E.E. Design, synthesis and antibacterial activity of coumarin-1,2,3-triazole hybrids obtained from natural furocoumarin peucedanin. *Molecules* **2019**, *24*, 2126. [CrossRef] [PubMed]
25. Lipeeva, A.V.; Khvostov, M.V.; Baev, D.S.; Shakirov, M.M.; Tolstikova, T.G.; Shults, E.E. Synthesis, *in vivo* anticoagulant evaluation and molecular docking studies of bicoumarins obtained from furocoumarin peucedanin. *Med. Chem.* **2016**, *12*, 674–683. [CrossRef]
26. Ivanov, A.A.; Ukladov, E.A.; Kremis, S.A.; Sharapov, S.Z.; Baiborodin, S.I.; Lipeeva, A.V.; Shults, E.E.; Golubeva, T.S. Investigation of cytotoxic and antioxidative activity of 1,2,3-triazolyl-modified furocoumarins and 2,3-dihydrofurocoumarins. *Protoplasma* **2022**, *259*, 1321–1330. [CrossRef]

27. Pramitha, P.; Bahulayan, D. Stereoselective synthesis of bio-hybrid amphiphiles of coumarin derivatives by Ugi–Mannich triazole randomization using copper catalyzed alkyne azide click chemistry. *Bioorg. Med. Chem. Lett.* **2012**, *22*, 2598–2603. [CrossRef]
28. Raposo, C.D.; Conceição, C.A.; Barros, M.T. Nanoparticles based on novel carbohydrate-functionalized polymers. *Molecules* **2020**, *25*, 1744. [CrossRef]
29. Jaabil, G.; Ranganathan, R.; Ponnuswamy, A.; Suresh, P.; Shanmugaiah, V.; Ravikumar, C.; Murugavel, S. A Green and efficient synthesis of bioactive 1,2,3-triazolyl-pyridine/cyanopyridine hybrids *via* one-pot multicomponent grinding protocol. *ChemistrySelect* **2018**, *3*, 10388–10393. [CrossRef]
30. Berger, O.; Kaniti, A.; Tran van Ba, C.; Vial, H.; Ward, S.A.; Biagini, G.A.; Bray, P.G.; O'Neill, P.M. Synthesis and antimalarial activities of a diverse set of triazole-containing furamidine analogues. *Chem. Med. Chem.* **2011**, *6*, 2094–2108. [CrossRef]
31. Mohamed, Z.H.; El-Koussi, N.A.; Mahfouz, N.M.; Youssef, A.F.; Jaleel, G.A.A.; Shouman, S.A. Cu (I) catalyzed alkyne-azide 1,3-dipolar cycloaddition (CuAAC): Synthesis of 17α-[1-(substituted phenyl)-1,2,3-triazol-4-yl]-19-nortestosterone-17β-yl acetates targeting progestational and antiproliferative activities. *Eur. J. Med. Chem.* **2015**, *97*, 75–82. [CrossRef]
32. Bottaro, C.; Penwell, P.E.; Schmitt, R.J. Expedient synthesis of *t*-butyl azide. *Synth. Commun.* **1997**, *27*, 1465–1467. [CrossRef]
33. Saikia, B.; Saikia, P.P.; Goswami, A.; Barua, N.C.; Saxena, A.K.; Suri, N. Synthesis of a novel series of 1,2,3-triazole-containing artemisinin dimers with potent anticancer activity involving Huisgen 1,3-dipolar cycloaddition reaction. *Synthesis* **2011**, *2011*, 3173–3179. [CrossRef]
34. Mosmann, T. Rapid colorimetric assay for cellular growth and survival: Application to proliferation and cytotoxicity assays. *J. Immunol. Methods* **1983**, *16*, 55–63. [CrossRef]
35. Nurmaganbetov, Z.S.; Savelyev, V.A.; Gatilov, Y.V.; Nurkenov, O.A.; Seidakhmetova, R.B.; Shulgau, Z.T.; Mukusheva, G.K.; Fazylov, S.D.; Shults, E.E. Synthesis and analgesic activity of 1-[(1,2,3-triazol-1-yl)methyl]quinolizines based on the alkaloid lupinine. *Chem. Heterocycl. Compd.* **2021**, *57*, 911–919. [CrossRef]
36. Finke, A.O.; Pavlova, A.V.; Morozova, E.A.; Tolstikova, T.G.; Shults, E.E. Synthesis of 1,2,3-triazolyl-substituted derivatives of the alkaloids sinomenine and tetrahydrothebaine on ring A and their analgesic activity. *Chem. Nat. Compd.* **2022**, *58*, 895–902. [CrossRef]
37. Schepetkin, I.A.; Nurmaganbetov, Z.S.; Fazylov, S.D.; Nurkenov, O.A.; Khlebnikov, A.I.; Seilkhanov, T.M.; Kishkentaeva, A.S.; Shults, E.E.; Quinn, M.T. Inhibition of acetylcholinesterase by novel lupinine derivatives. *Molecules* **2023**, *28*, 3357. [CrossRef]
38. Burlison, J.A.; Blagg, B.S. Synthesis and evaluation of coumermycin A1 analogues that inhibit the Hsp90 protein folding machinery. *Org. Lett.* **2006**, *8*, 4855–4858.
39. Kusuma, B.R.; Peterson, L.B.; Zhao, H.; Vielhauer, G.; Holzbeierlein, J.; Blagg, B.S.J. Targeting the heat shock protein 90 dimer with dimeric inhibitors. *J. Med. Chem.* **2011**, *54*, 6234–6253. [CrossRef]
40. Tan, G.; Yao, Y.; Gu, Y.; Li, S.; Lv, M.; Wang, K.; Chen, H.; Li, X. Cytotoxicity and DNA binding property of the dimers of triphenylethylene–coumarin hybrid with one amino side chain. *Bioorg. Med. Chem. Lett.* **2014**, *24*, 2825–2830. [CrossRef]
41. Creary, X.; Anderson, A.; Brophy, C.; Crowell, F.; Funk, Z. Method for assigning structure of 1,2,3-triazoles. *J. Org. Chem.* **2012**, *77*, 8756–8761. [CrossRef] [PubMed]
42. Dhawan, S.; Singh, A.; Manhas, N.; Seboletswe, P.; Khubone, L.; Kumar, G.; Jonnalagadda, S.B.; Raza, A.; Sharma, A.K.; Singh, P. Exploring novel coumarin-tethered bis-triazoles: Apoptosis induction in human pancreatic cancer cells, antimicrobial effects, and molecular modelling investigations. *ChemMedChem* **2024**, *19*, e202400297. [CrossRef] [PubMed]
43. Al-Warhi, T.; Sabt, A.; Elkaeed, E.B.; Eldehna, W.M. Recent advancements of coumarin-based anticancer agents: An up-to-date review. *Bioorg. Chem.* **2020**, *103*, 104163. [CrossRef]
44. Yadav, A.K.; Shrestha, R.M.; Yadav, P.N. Anticancer mechanism of coumarin-based derivatives. *Eur. J. Med. Chem.* **2024**, *267*, 116179. [CrossRef]
45. Pfeffer, C.M.; Singh, A.T.K. Apoptosis: A target for anticancer therapy. *Int. J. Mol. Sci.* **2018**, *19*, 448. [CrossRef] [PubMed]
46. Wong, R.S.J. Apoptosis in cancer: From pathogenesis to treatment. *J. Exper. Clin. Cancer Res.* **2011**, *30*, 87. [CrossRef]
47. Nagy, N.; Kuipers, H.F.; Frymoyer, A.R.; Ishak, H.D.; Bollyky, J.B.; Wight, T.N.; Bollyky, P.L. 4-Methylumbelliferone treatment and hyaluronan inhibition as a therapeutic strategy in inflammation, autoimmunity, and cancer. *Front. Immunol.* **2015**, *6*, 123. [CrossRef]
48. Martin, S.J. Cell death and inflammation: The case for IL-1 family cytokines as the canonical DAMPs of the immune system. *FEBS J.* **2016**, *283*, 2599–2615. [CrossRef]

Disclaimer/Publisher's Note: The statements, opinions and data contained in all publications are solely those of the individual author(s) and contributor(s) and not of MDPI and/or the editor(s). MDPI and/or the editor(s) disclaim responsibility for any injury to people or property resulting from any ideas, methods, instructions or products referred to in the content.